scientific reports

Check for updates

OPEN

Anti-fibrogenic effect of umbilical cord–derived mesenchymal stem cell–conditioned media in human esophageal fibroblasts

Yoon Jeong Choi[1,2,4], Jee Hyun Kim[1,4], Yeonju Lee[1], Hee Jang Pyeon[3], In Kyung Yoo[1]✉ & Jun Hwan Yoo[1,2]✉

Esophageal fibrosis can develop due to caustic or radiation injuries. Umbilical cord–derived mesenchymal stem cells (UC-MSCs) are known to mitigate fibrosis in various organs. However, the potential effects of UC-MSCs on human esophageal fibrosis remain underexplored. This study investigated the anti-fibrogenic properties and mechanisms of UC-MSC-derived conditioned media (UC-MSC-CM) on human esophageal fibroblasts (HEFs). HEFs were treated with TGF-β1 and then cultured with UC-MSC-CM, and the expression levels of extracellular matrix (ECM) components, RhoA, myocardin related transcription factor A (MRTF-A), serum response factor (SRF), Yes-associated protein (YAP), and transcriptional coactivator with PDZ-binding motif (TAZ) were measured. UC-MSC-CM suppressed TGF-β1-induced fibrogenic activation in HEFs, as evidenced by the downregulation of ECM. UC-MSC-CM diminished the expression of RhoA, MRTF-A, and SRF triggered by TGF-β1. In TGF-β1-stimulated HEFs, UC-MSC-CM decreased the nuclear localization of MRTF-A and YAP. Additionally, UC-MSC-CM diminished the TGF-β1-induced nuclear expressions of YAP and TAZ, while concurrently enhancing the cytoplasmic presence of phosphorylated YAP. Furthermore, UC-MSC-CM reduced TGF-β1-induced phosphorylation of Smad2. These findings suggest that UC-MSC-CM may inhibit TGF-β1-induced fibrogenic activation in HEFs by targeting the Rho-mediated MRTF/SRF and YAP/TAZ pathways, as well as the Smad2 pathway. This indicates its potential as a stem cell therapy for esophageal fibrosis.

Keywords Esophageal fibrosis, Mesenchymal stem cells, Umbilical cord, Conditioned medium

Esophageal fibrosis and strictures commonly observed in clinical practice are often a consequence of caustic injuries, radiation exposure, or surgical procedures, such as endoscopic submucosal dissection[1]. Their pathogenesis involves severe inflammation, scar formation, and fibrosis, marked by excessive extracellular matrix (ECM) deposition, especially collagen, which leads to tissue hardening and narrowing of the esophageal lumen. Steroids, administered orally or locally, are the predominant therapeutic option; however, are hindered by limited efficacy and risk of immunosuppression and infection[2]. This lack of effective anti-fibrotic agents highlights a critical gap in the treatment of esophageal strictures.

The role of transforming growth factor-beta (TGF-β) as a critical pro-fibrotic cytokine promoting fibrogenic activity in myofibroblasts has been well established in fibrosis research. TGF-β1 operates through two primary pathways: the Smad-dependent and Smad-independent pathways[3–5]. In the Smad-dependent pathway, TGF-β1 induction leads to the phosphorylation and nuclear translocation of Smad2 and Smad3, initiating the transcription of pro-fibrotic genes[3,4]. Alternatively, the Smad-independent pathway involves the RhoA/ Rho-associated protein kinase (ROCK) pathway, which is crucial for the regulation of fibrosis[4,5]. Another Smad-independent TGF-β signaling is transduced by phosphorylation of extracellular signal-regulated kinase (ERK), c-Jun N-terminal kinase (JNK), p38 mitogen-activated protein kinase (MAPK), and AKT[4,6].

[1]Department of Gastroenterology, CHA Bundang Medical Center, CHA University School of Medicine, 59 Yatap-ro, Bundang-gu, Seongnam 13496, South Korea. [2]Institute of Basic Medical Sciences, CHA University School of Medicine, Seongnam 13496, South Korea. [3]R&D Division, CHA Biotech Co., Ltd, Seongnam 13488, South Korea. [4]Yoon Jeong Choi and Jee Hyun Kim contributed equally to this work. ✉email: ikyoo82@hanmail.net; jhyoo@cha.ac.kr

As for the RhoA/ROCK pathway, the transcriptional regulators Yes-associated protein (YAP) and transcriptional co-activator with PDZ-binding motif (TAZ/WWTR1), which are integral to the Hippo signaling pathway, have been implicated in the pathogenesis of fibrosis across a variety of organs[7–11]. This modulation is primarily achieved through the dephosphorylation of YAP/TAZ, which is a critical step in activating YAP/TAZ signaling, thereby influencing cellular responses related to fibrosis[12].

Recent advances in regenerative medicine, particularly those involving mesenchymal stem cells (MSCs), have opened new avenues for treating various diseases, including those affecting the digestive tract[13]. Umbilical cord–derived stem cells (UC-MSCs) offer distinct advantages over other MSC sources[13], including their abundant availability, lack of ethical controversy, superior proliferative capacity, and potentially greater efficacy in clinical applications[14].

However, despite the therapeutic potential of MSCs, direct cellular therapies present challenges because of concerns about vascular obstruction, the potential for malignant transformation, and issues related to cell survival and integration[15–17]. The growing interest in MSC-conditioned media (CM) stems from its rich composition of biologically active molecules and extracellular vesicles (EVs). CM is a source of critical enzymes involved in ECM remodeling, notably matrix metalloproteinases (MMP2 and MMP9) and their inhibitors, TIMP-1 and TIMP-2. Additionally, it contains anti-fibrogenic cytokines, such as interleukin-10 (IL-10) and prostaglandin-E2, along with growth factors, such as vascular endothelial growth factor and hepatocyte growth factor. CM derived from human UC-MSC (UC-MSC-CM) has demonstrated significant anti-fibrotic effects in various organ systems[14,18–20].

Therefore, this study aimed to identify the inhibitory effect of UC-MSC-CM on the fibrogenic activation of human esophageal fibroblasts (HEFs) and to determine the intracellular mechanisms involved in the inhibitory effect.

Results

UC-MSC-CM inhibits TGF-β1-induced ECM and α-SMA expression in HEFs

To determine whether UC-MSC-CM inhibits the activation of the fibrogenic process in fibroblasts, HEFs were cultured with UC-MSC-CM and simultaneously stimulated with TGF-β1. The mRNA expression of *COL1A1*, *FN1*, and *ACTA2* (encoding Collagen1A1, FN, and α-SMA, respectively) was significantly elevated by TGF-β1 in the HEFs. This effect was decreased by culture with UC-MSC-CM (Fig. 1A). The anti-fibrogenic effect of UC-MSC-CM was also observed at the level of protein expression. The TGF-β1-induced upregulation of Procol1A1, FN, and α-SMA protein expression was significantly reduced in a concentration-dependent manner when cultured with UC-MSC-CM (Fig. 1B,C; Fig. S1).

α-SMA immunostaining revealed well-organized, brightly stained actin stress fibers, and Procol1A1 and FN immunostaining also exhibited high signals in TGF-β1-stimulated cells (Fig. 2A,B). In contrast, cells exposed to UC-MSC-CM displayed reduced staining of Procol1A1 and FN, as well as diffuse and muted α-SMA staining with lacked structured stress fibers that resembled the control group (Fig. 2B). These findings suggest that UC-MSC-CM inhibits the activation of the TGF-β1-induced fibrogenic process in HEFs by downregulating the mRNA and protein expression of ECM and α-SMA.

UC-MSC-CM inhibits Rho/MRTF/SRF signaling in HEFs

In our previous study, we showed that UC-MSCs suppress the TGF-β1-induced synthesis of ECM and α-SMA in human intestinal myofibroblasts by blocking Rho/MRTF/SRF signaling[7]. Therefore, we examined whether UC-MSC-CM reduced the TGF-β1-induced expression of Procol1A1, FN, and α-SMA in HEFs via the same mechanism. The expression of *MRTFA* and *SRF* mRNA elicited by TGF-β1 was significantly reduced by UC-MSC-CM in a dose-dependent manner (Fig. 3A). We also examined the expression of *RHOA*, *ROCK1*, *ROCK2*, and *SRC*, which are upstream molecules of the MRTF/SRF pathway involved in the polymerization of F-actin, a process that is crucial for fibrogenesis[10]. UC-MSC-CM reduced the TGF-β1-induced mRNA expression levels of *RHOA* and *SRC* in the HEFs (Fig. 3A). Although not statistically significant, UC-MSC-CM induced a decreasing trend in *ROCK1* expression. Compared with TGF-β1 treatment alone, UC-MSC-CM culture decreased *ROCK2* mRNA expression, which was not stimulated by TGF-β1. At the protein level, UC-MSC-CM significantly decreased the TGF-β1-induced expression of MRTF-A and SRF in nuclear extracts as well as RhoA in cytoplasmic extracts (Fig. 3B,C; Fig. S2).

In addition, we measured the nuclear-to-cytoplasmic signal ratio via immunohistochemical analysis of MRTF-A to further assess whether the inhibition of MRTF-A nuclear localization is also involved in the anti-fibrogenic mechanism of UC-MSC-CM. The nuclear-to-cytoplasmic signal ratio of MRTF-A in unstimulated and TGF-β1-stimulated cells showed no significant difference. However, in TGF-β1-stimulated cells, treatment with UC-MSC-CM led to a significant reduction in the nuclear localization of MRTF-A (Fig. 4A,B).

In Fig. 4A (j, k, l), the signal intensity of MRTF-A in cytoplasm appeared to be increased after UC-MSC-CM. Therefore, we performed the additional western blotting to detect MRTF-A in the cytoplasmic fraction to investigate whether the reduction of nuclear/cytoplasmic ratio of MRTF-A was due to its overall increased expression in the cytosol. We found that the protein expression of MRTF-A in the cytoplasmic extracts was significantly increased after UC-MSC-CM treatment compared with TGF-β1 treatment alone (Fig. S3). we have already shown that the protein expression of MRTF-A in the nuclear extracts was significantly reduced after UC-MSC-CM treatment (Fig. 3B,C). Taken together, the reduction of nuclear/cytoplasmic ratio of MRTF-A after UC-MSC-CM treatment appears to be due to combined effect of its decreased expression in the nucleus as well as its increased expression in the cytosol.

We then stained F-actin with rhodamine-phalloidin to ascertain whether UC-MSC-CM affected F-actin polymerization, which occurs upstream of MRTF-A/SRF signaling and downstream of Rho/ROCK signaling in HEFs. TGF-β1-stimulated cells showed enhanced F-actin staining, indicating F-actin polymerization (stress

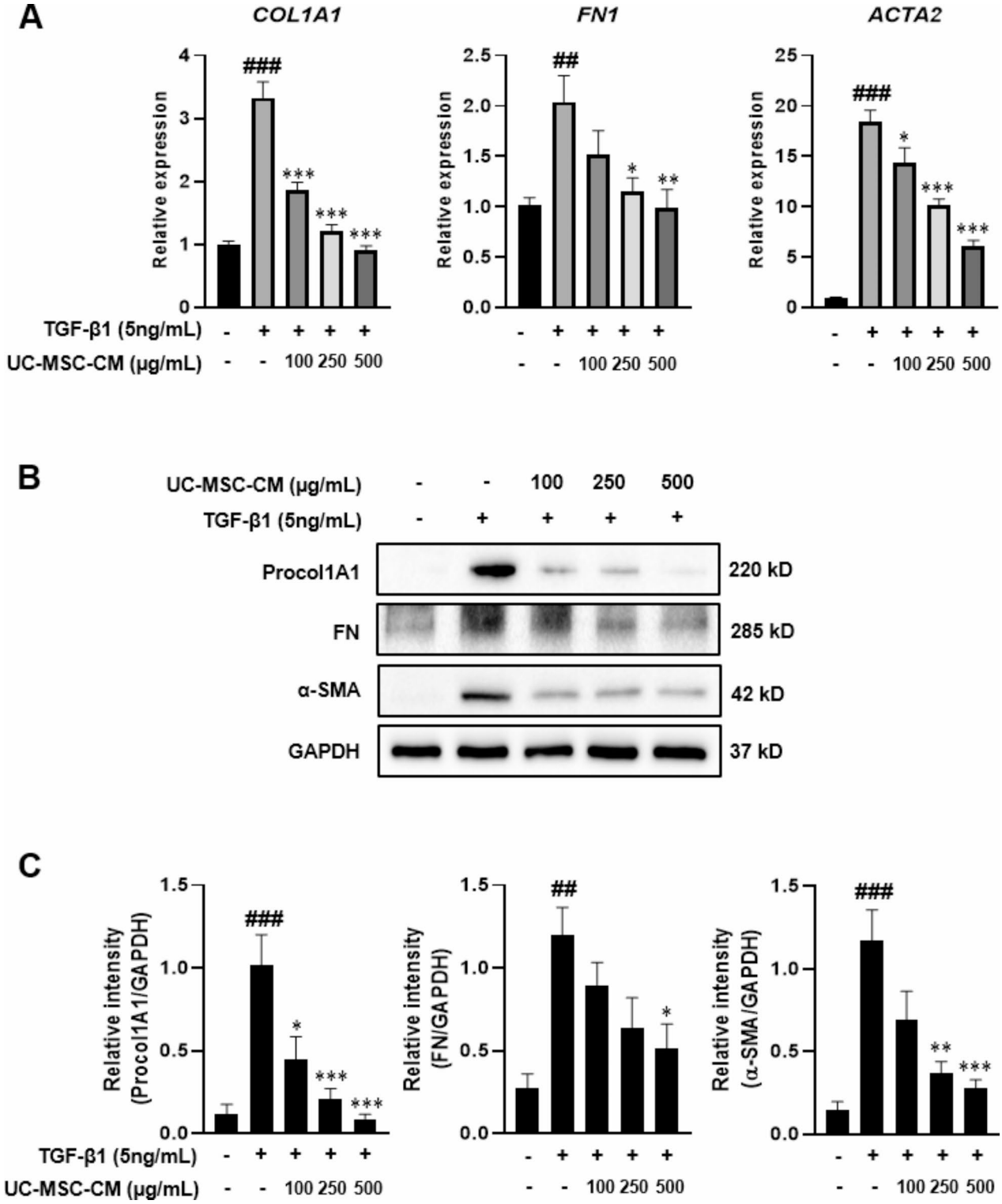

Fig. 1. Culture with umbilical cord–derived mesenchymal stem cell–conditioned media (UC-MSC-CM) inhibits the TGF-β1-induced fibrogenic activation process in human esophageal fibroblasts (HEFs). HEFs were treated with TGF-β1 (5 ng/mL) and cultured with or without UC-MSC-CM (24 h for RT-qPCR analysis, 48 h for western blotting). (**A**) RT-qPCR analysis of the relative mRNA expression of collagen1A1 (COL1A1), fibronectin (FN1), and α-smooth muscle actin (ACTA2). Data were normalized to GAPDH expression and expressed as relative values compared to the control (n = 4). (**B**) Representative western blots showing the protein expression of procollagen1A1 (Procol1A1), fibronectin (FN) and α-smooth muscle actin (α-SMA), with GAPDH as a loading control. (**C**) Quantitation of Procol1A1, FN, and α-SMA levels from western blot analyses (n = 4). Data are expressed as the mean ± SEM. $^{\#\#}P < 0.01$ and $^{\#\#\#}P < 0.001$ versus the control; $^{*}P < 0.05$, $^{**}P < 0.01$, and $^{***}P < 0.001$ versus TGF-β1 treatment only (ANOVA w/ Tukey). Original images of blots are presented in Supplementary Fig. S1.

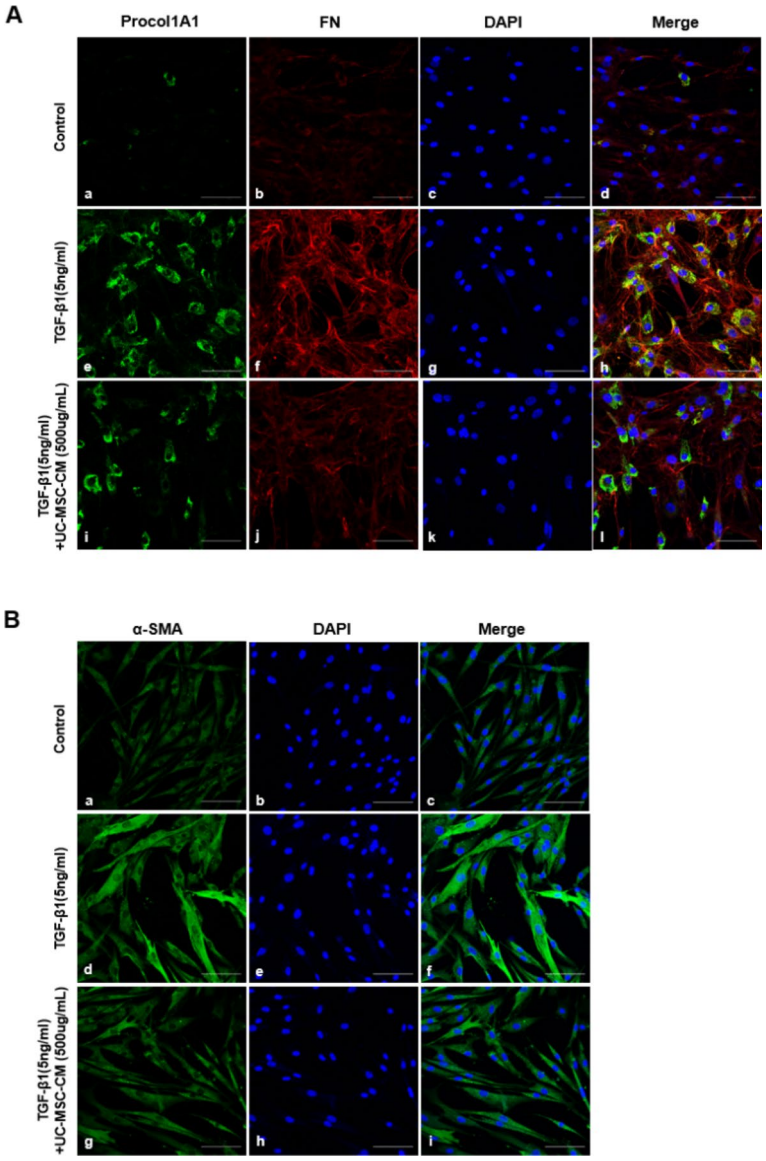

Fig. 2. Culture with UC-MSC-CM inhibits TGF-β1-induced Procol1A1, FN, and α-SMA expression in HEFs. HEFs were treated with TGF-β1 (5 ng/mL) and cultured with or without UC-MSC-CM for 48 h and then stained with Procol1A1 and FN (**A**) and α-SMA (**B**) antibodies and counterstained with DAPI. Scale bars, 100 μm; original magnification, ×200.

fiber production), in comparison with that in the controls (Fig. 4C). However, UC-MSC-CM reduced the F-actin production induced by TGF-β1. Analysis of intensity ratio of F-actin to DAPI also showed a statistically significant increase in fluorescence intensity by TGF-β1 treatment and this effect was significantly reduced by UC-MSC-CM (Fig. 4D). Collectively, these findings imply that Rho/MRTF/SRF signaling in HEFs may be inhibited by UC-MSC-CM.

UC-MSC-CM inhibits YAP/TAZ signaling in HEFs

The TGF-β1-induced expression of *WWTR1* was significantly reduced by UC-MSC-CM in a dose-dependent manner (Fig. 5A). Although *YAP1* expression tended to decrease, the reduction was not statistically significant. The anti-fibrogenic effect of UC-MSC-CM was also identified at the protein level. The TGF-β1-induced protein expression of YAP and TAZ in nuclear extracts was significantly reduced in proportion to the concentration by culture with UC-MSC-CM (Fig. 5B,C; Fig. S4). However, phosphorylated YAP (p-YAP) in cytoplasmic extracts, which was initially reduced significantly by TGF-β1, was increased by UC-MSC-CM in a dose-dependent manner (Fig. 5B,C; Fig. S4). Quantitative analyses were conducted using immunohistochemistry to determine the nuclear-to-cytoplasmic signal ratio of YAP. This study was undertaken to elucidate the consequence of inhibiting YAP nuclear localization in the anti-fibrogenic mechanism mediated by UC-MSC-CM. Notably, we observed a marked elevation in the nuclear-to-cytoplasmic signal ratio of YAP in HEFs following stimulation with TGF-β1. Conversely, in TGF-β1-stimulated HEFs, exposure to UC-MSC-CM resulted in a statistically

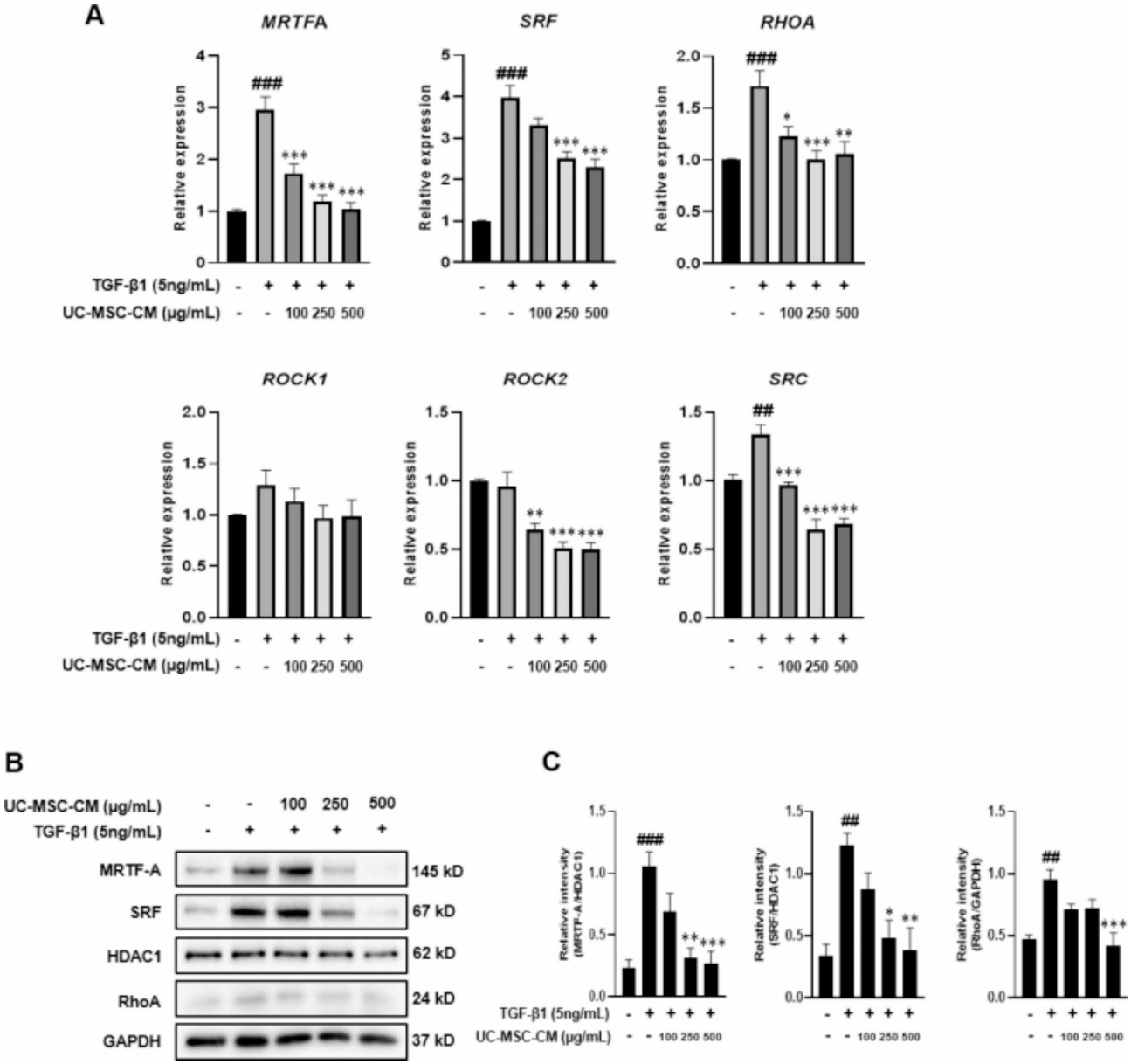

Fig. 3. UC-MSC-CM inhibits Rho/MRTF/SRF signaling in HEFs. HEFs were treated with TGF-β1 (5 ng/mL) and cultured with or without UC-MSC-CM (24 h for RT-qPCR analysis, 48 h for western blotting). (**A**) RT-qPCR analysis of the relative mRNA expression of MRTFA, SRF, RHOA, ROCK1, ROCK2, and SRC. Data were normalized to GAPDH expression and expressed as relative values compared to the control (n = 3). (**B**) Representative western blots showing the protein expression of MRTF-A and SRF in the nuclear extracts with histone deacetylase (HDAC1) as a loading control, and RhoA in the cytoplasmic extracts with GAPDH as a loading control. (**C**) Quantitation of MRTF-A, SRF, and RhoA from western blot analyses (n = 4). Data are expressed as the mean ± SEM. $^{\#\#}P < .01$ and $^{\#\#\#}P < 0.001$ versus the control; *P < 0.05, **P < 0.01, and ***P < 0.001 versus TGF-β1 treatment only (ANOVA w/ Tukey). Original images of blots are presented in Supplementary Fig. S2.

significant attenuation of YAP nuclear localization (Fig. 6A,B). To validate this finding using a more quantitative approach, we conducted additional western blotting to detect YAP in the cytoplasmic fraction (Fig. S3). Interestingly, the protein expression of YAP in the cytoplasmic extracts showed no significant change after UC-MSC-CM treatment. We previously showed that YAP protein expression in the nuclear extracts was significantly reduced following UC-MSC-CM treatment. In contrast, the expression of p-YAP in the cytoplasmic extracts was significantly increased with UC-MSC-CM treatment compared to TGF-β1 treatment alone (Fig. 5B,C). These findings suggest that, in response to TGF-β1, YAP detaches from the phosphate group and translocates to the nucleus; however, this process is significantly inhibited by UC-MSC-CM. Taken together, the reduction in the nuclear/cytoplasmic ratio of YAP after UC-MSC-CM treatment appears to result from a combined effect of decreased nuclear expression of YAP and increased cytoplasmic p-YAP expression. Collectively, these findings

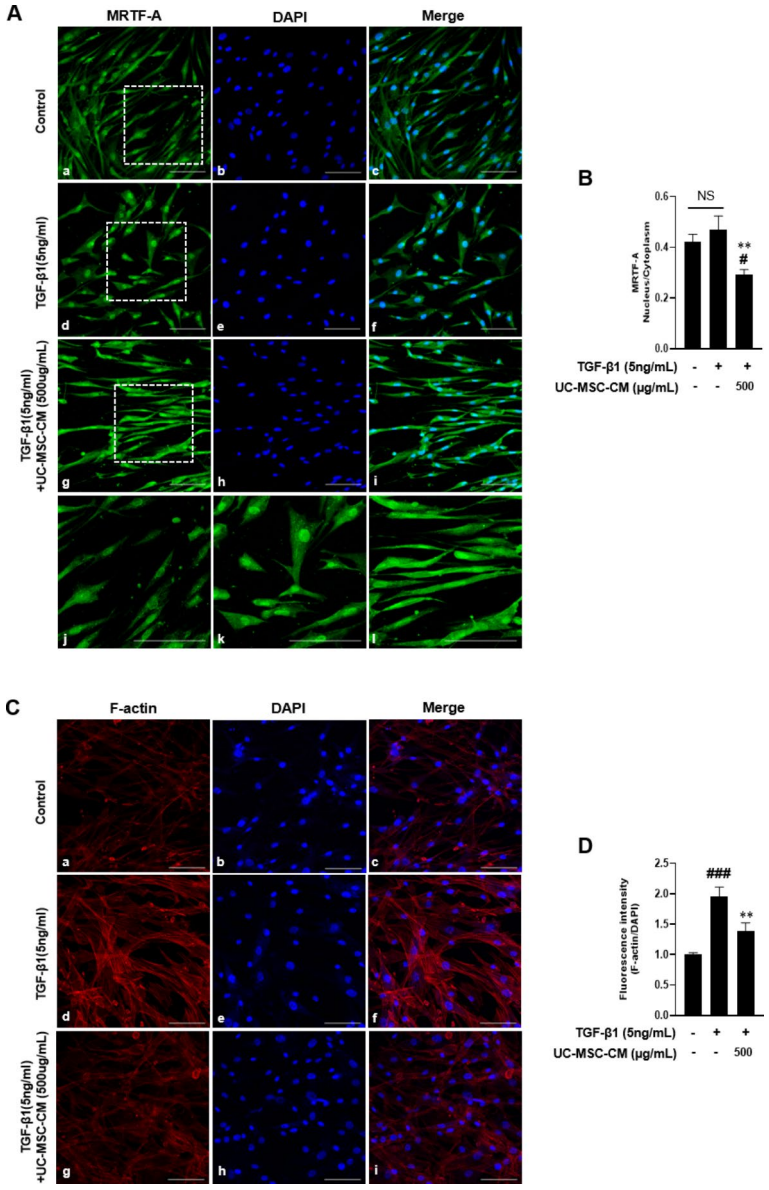

Fig. 4. UC-MSC-CM inhibits MRTF-A nuclear localization in HEFs. HEFs were treated with TGF-β1 (5 ng/mL) and cultured with or without UC-MSC-CM for 48 h and then stained with MRTF-A antibody (**A**), rhodamine-phalloidin (**C**), and counterstained with DAPI. (**A**) (**a**–**c**) no treatment; (**d**–**f**) treatment with TGF-β1; (**g**–**i**) treatment with TGF-β1 and UC-MSC-CM; (**j**–**l**) enlarged images of the region within the white box in (**a**), (**d**) and (**g**), respectively. (**B**) Nuclear-to-cytoplasmic ratio of MRTF-A was determined for each condition as described in "Methods" section. (**D**) The fluorescence intensity ratio of F-actin to DAPI was quantified and plotted using ImageJ software: Measurements were taken across 21 distinct same sized surface areas (3900 μm ^{2} for images taken with zoom factor 1) from 3 independent experiments. Data are expressed as the mean ± SEM. $^{\#}P < 0.05$ and $^{\#\#\#}P < 0.001$ versus the control; $^{**}P < 0.01$ versus TGF-β1 treatment only (ANOVA w/ Tukey). *NS* not significant (Mann–Whitney U test); Scale bars, 100 μm; original magnification, ×200.

suggest that UC-MSC-CM inhibits the fibrogenic activation of HEFs induced by TGF-β1 by downregulating YAP/TAZ signaling.

UC-MSC-CM decreases the TGF-β1-induced phosphorylation of Smad2

We also investigated the involvement of classical Smad-dependent TGF-β pathways in the anti-fibrogenic mechanism of UC-MSC-CM in HEFs. UC-MSC-CM significantly reduced the TGF-β1-induced Smad2 phosphorylation in a dose-dependent manner (Fig. 7A,B; Fig. S5). These findings imply that the anti-fibrogenic effects of UC-MSC-CM are mediated through Smad-dependent mechanisms.

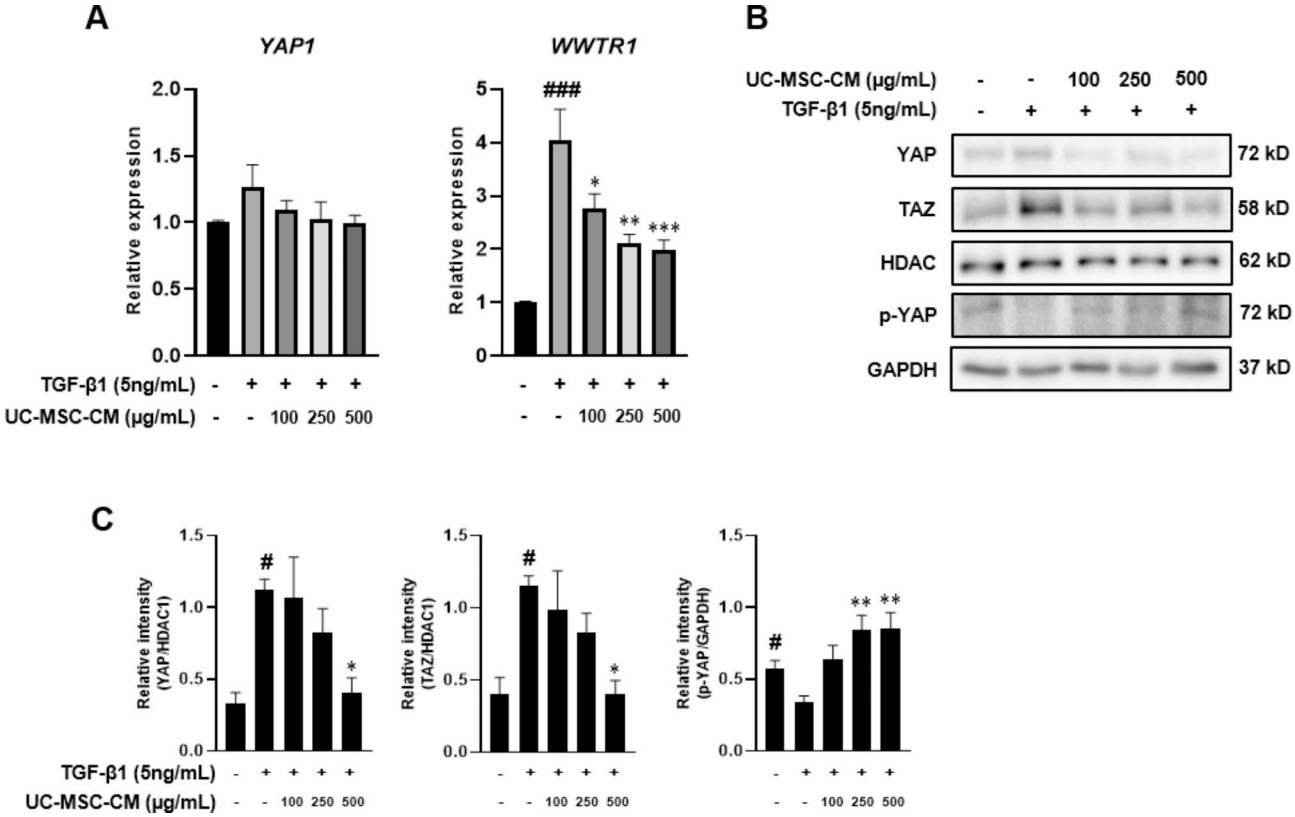

Fig. 5. UC-MSC-CM inhibits YAP/TAZ signaling in HEFs. HEFs were treated with TGF-β1 (5 ng/mL) and cultured with or without UC-MSC-CM (24 h for RT-qPCR analysis, 48 h for western blotting). (**A**) RT-qPCR analysis of the relative mRNA expression of YAP1 and WWTR1. Data were normalized to GAPDH expression and expressed as relative values compared to the control (n = 3). (**B**) Representative western blots showing the protein expression of YAP and TAZ in the nuclear extracts with histone deacetylase (HDAC1) as a loading control, and p-YAP in the cytoplasmic fraction with GAPDH as a loading control. (**C**) Quantitation of YAP, TAZ, and p-YAP from western blot analyses (n = 4 except for p-YAP (n = 6)). Data are expressed as the mean ± SEM. $^{\#}P < 0.05$, $^{\#\#}P < 0.01$, and $^{\#\#\#}P < 0.001$ versus the control; $^{*}P < 0.05$, $^{**}P < 0.01$, and $^{***}P < 0.001$ versus TGF-β1 treatment only (ANOVA w/ Tukey). Original images of blots are presented in Supplementary Fig. S4.

Discussion

This study highlights the therapeutic potential of UC-MSC-CM for the treatment of esophageal fibrosis. Our findings demonstrate that UC-MSC-CM effectively inhibited fibrogenic activation in HEFs induced by TGF-β1, a key cytokine implicated in the pathogenesis of fibrosis. UC-MSC-CM attenuated the TGF-β1-induced expression of fibrogenic markers, such as collagen1A1, FN, and α-SMA, at both the mRNA and protein levels. Additionally, UC-MSC-CM suppressed activation of the Rho/MRTF/SRF signaling pathway by reducing the expression of RhoA, ROCK2, F-actin, MRTF-A, and SRF, as well as the nuclear localization of MRTF-A. Furthermore, UC-MSC-CM inhibited the YAP/TAZ signaling pathway by decreasing the expression of YAP and TAZ and increasing that of p-YAP. Finally, UC-MSC-CM reduced the TGF-β1-induced phosphorylation of Smad2, suggesting the involvement of Smad-dependent mechanisms in its action.

This study demonstrated that UC-MSC-CM inhibits the TGF-β1-induced fibrogenic activation process in HEFs by reducing the expression of ECM components (Procol1A1 and FN), which represent the final products of fibrogenesis. Additionally, UC-MSC-CM decreased the expression of α-SMA, which is a marker of contractile force[21]. These findings were consistent with those of previous studies highlighting the anti-fibrogenic effects of UC-MSC-CM in various organs, including the liver, heart, kidneys, and lungs. For example, in hepatic stellate cells, UC-MSC-CM reduced the expression of collagens and α-SMA, as well as the phosphorylation of Smad2, all of which are induced by TGF-β1[22].

Here, we found that UC-MSC-CM inhibited the fibrogenic activation process in HEFs by targeting the MRTF/SRF signaling axis, a Smad-independent pathway involved in fibrosis. In the nucleus, MRTF-A, a transcription co-activator, activates the SRF-dependent transcription of pro-fibrotic genes containing serum response elements in their promoters, including ECM and α-SMA[23] (Fig. 8). Our study revealed that culture with UC-MSC-CM attenuates the TGF-β1-induced expression of MRTF-A and SRF while inhibiting the nuclear translocation of MRTF-A, which is evident from increased cytoplasmic staining. Diminished nuclear localization of MRTF-A appeared to correlate with decreased F-actin polymerization, as shown by F-actin immunostaining.

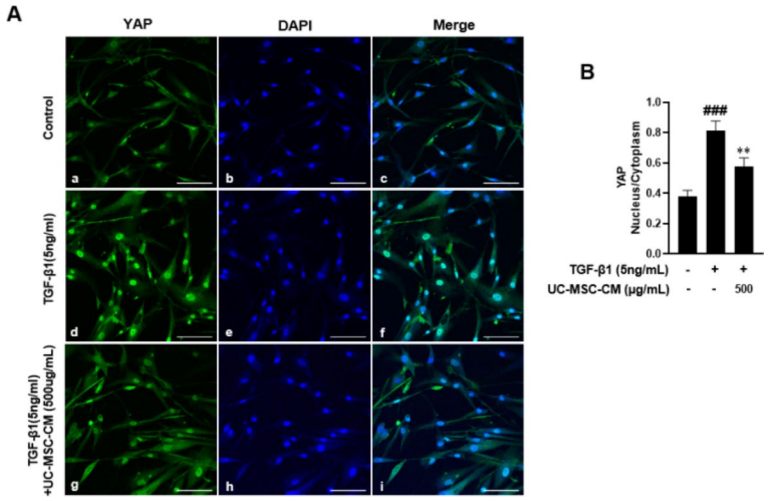

Fig. 6. Culture with UC-MSC-CM inhibits nuclear localization of YAP in HEFs. (**A**) HEFs were treated with TGF-β1 (5 ng/mL) and cultured with or without UC-MSC-CM for 48 h and then stained with YAP antibody and counterstained with DAPI. (**B**) Nuclear-to-cytoplasmic ratio of YAP was determined for each condition as described in "Methods" section. Data are expressed as the mean ± SEM. $^{###}P < 0.001$ versus the control; $^{**}P < 0.01$ versus TGF-β1 treatment only (ANOVA w/ Tukey). Scale bars, 100 μm; original magnification, ×200.

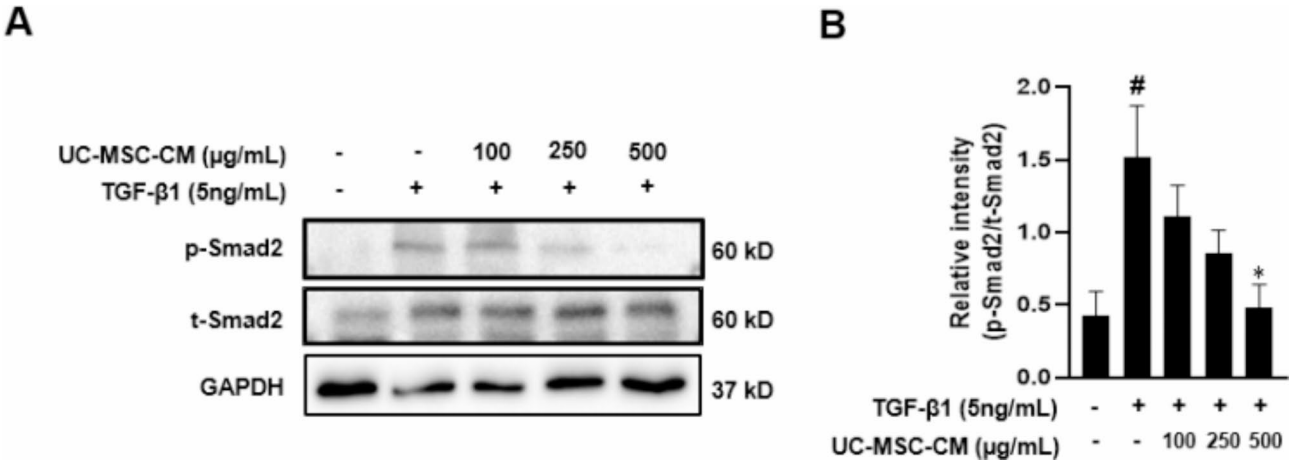

Fig. 7. UC-MSC-CM decreases the TGF-β1-induced phosphorylation of Smad2. HEFs were treated with TGF-β1 (5 ng/mL) and cultured with or without UC-MSC-CM for 48 h. (**A**) Representative western blots showing the protein expression of phosphorylated Smad2 (p-Smad2) and total Smad2 with GAPDH as a loading control. (**B**) Quantitation of p-Smad2 using western blot analyses (n = 4). Data are expressed as the mean ± SEM. $^{\#}P < 0.05$ versus the control; $^{*}P < 0.05$ versus TGF-β1 treatment only (ANOVA w/ Tukey). Original images of blots are presented in Supplementary Fig. S5.

The nuclear localization of MRTF has been reported to be influenced by cytoskeletal modifications, notably actin polymerization; however, the exact mechanism remains unclear[24]. This observation was consistent with our previous findings, in which UC-MSCs disrupted F-actin/MRTF/SRF signaling, thereby inhibiting the fibrogenic activation of human intestinal myofibroblasts[18].

YAP/TAZ signaling, known to promote fibrosis in multiple organs, including the liver, kidneys, and lungs[7–11], is a crucial pathway in the core fibrogenic process. The evolutionarily conserved Hippo pathway plays a critical role in various biological processes, including tissue and organ regeneration, homeostasis, and development. YAP and TAZ are pivotal components of the Hippo pathway[12,25,26] that modulate TGF-β1/Smad signaling by affecting the nuclear/cytoplasmic localization of Smad2/3. Activation of the Hippo pathway leads to the phosphorylation of YAP/TAZ by Lats 1/2 activation, resulting in their retention in the cytoplasm. This phosphorylated state of YAP/TAZ in the cytoplasm inhibits Smad2/3 nuclear localization[27]. Conversely, unphosphorylated YAP/TAZ, upon TGF-β1 stimulation, binds to Smad2/3 and mediates their nuclear localization[11,28,29]. Once localized in the nucleus, YAP/TAZ interacts with TGF-induced Smad2/3 to form the YAP/TAZ/TEAD/Smad2/3 complex,

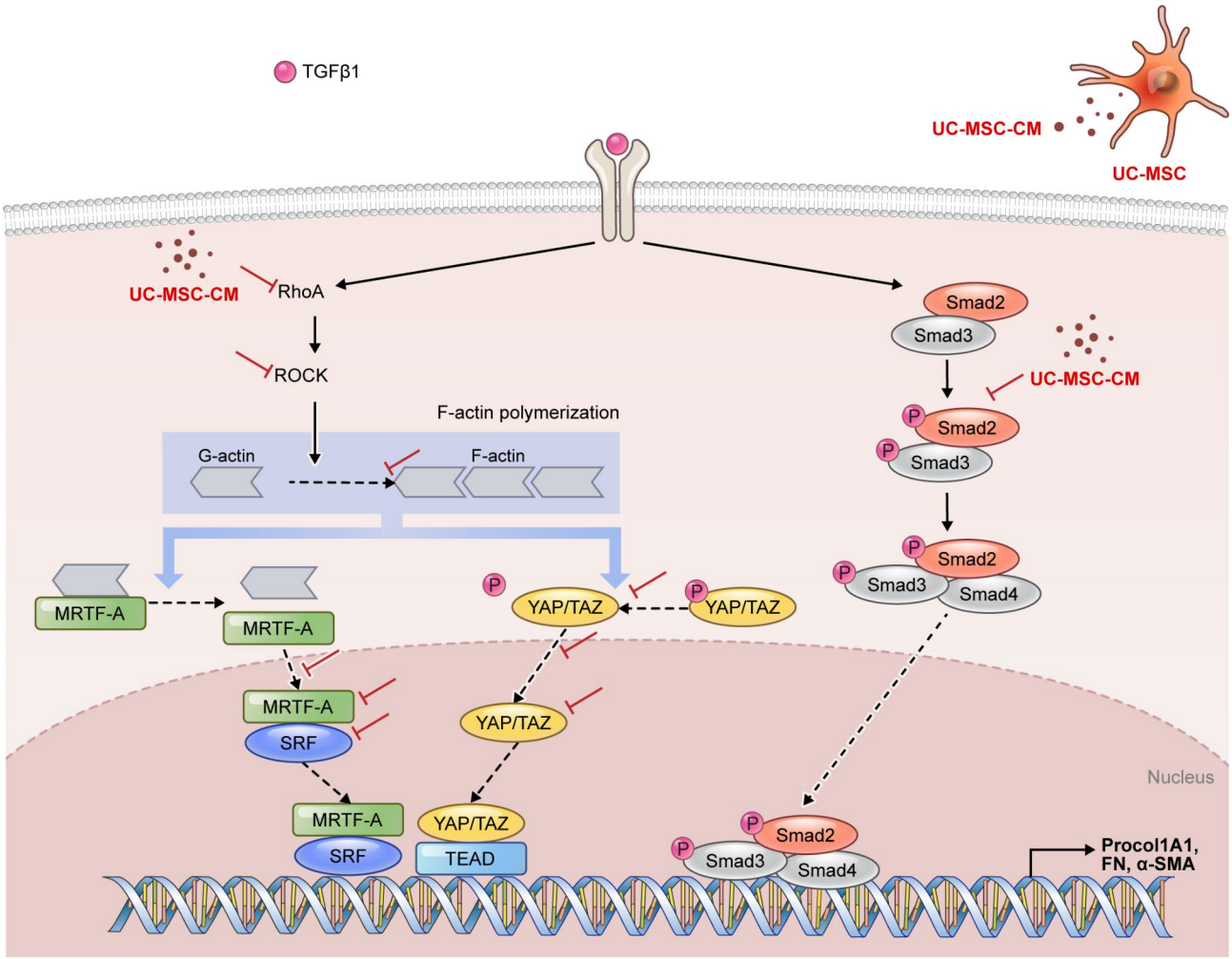

Fig. 8. Inhibition of TGF-β1-induced fibrogenic activation by UC-MSC-CM in HEFs. This model illustrates the cascade initiated by TGF-β1 binding to its receptor, which promotes RhoA activation that subsequently activates ROCK. Activation of the RhoA/ROCK pathway enhances G-actin polymerization into F-actin, releasing MRTF-A from G-actin, which then translocates into the nucleus. Concurrently, RhoA-driven F-actin polymerization leads to YAP/TAZ dephosphorylation and their nuclear translocation. In the nucleus, MRTF-A, YAP, and TAZ serve as transcriptional co-activators with SRF or TEAD to upregulate fibrogenic genes such as Procol1A1, FN, and α-SMA. Additionally, TGF-β1 induces phosphorylation of Smad2/3, which then bind to Smad4 and translocate into the nucleus, where they induce fibrosis. UC-MSC-CM is depicted as interfering with TGF-β1 signal transduction by impeding the Smad 2 pathway and the RhoA-mediated MRTF-A/SRF and YAP/TAZ pathways, thereby attenuating fibrogenic gene transcription.

which regulates various TGF-induced transcription activities. The interaction between YAP/TAZ and TEAD transcription factors has been linked to numerous functions, including immunological regulation, tissue regeneration, epithelial homeostasis, wound healing, and organ development[30]. Furthermore, YAP/TAZ enhances matrix remodeling and promotes fibroblast development.

In this study, we found that the anti-fibrogenic effects of UC-MSC-CM in HEFs were mediated through the YAP/TAZ signaling pathway. Culture with UC-MSC-CM suppressed YAP/TAZ expression in the nucleus and increased YAP phosphorylation in the cytosol of HEFs. Furthermore, UC-MSC-CM inhibited its nuclear translocation, as evidenced by enhanced staining of YAP in the cytoplasmic compartment, indicating a shift in YAP localization from the nucleus to the cytoplasm. Dysregulation of the YAP/TAZ pathway has been increasingly recognized as a pivotal element in the progression of pulmonary fibrosis, emphasizing its potential as a target for novel therapeutic interventions[31].

In our investigation, we focused on determining whether UC-MSC-CM influences upstream molecules in the MRTF/SRF and YAP/TAZ pathways. Therefore, we analyzed the expression levels of RhoA, ROCK1, ROCK2, and SRC in HEFs. The Rho/ROCK signaling cascade is integral to the activation of MRTF/SRF transcription[32]. Various biochemical and physical factors, such as TGF-β1, matrix stiffness, and G protein-coupled receptor ligands, stimulate RhoA GTPase activity. RhoA promotes F-actin polymerization through the activation of downstream effectors, namely ROCK and mammalian diaphanous (mDia). This process occurs in two key

steps: first, ROCK facilitates LIM kinase-dependent inhibition of F-actin depolymerization; second, RhoA promotes mDia-dependent F-actin polymerization. Notably, SRC also activates mDia. As crucial mediators of signal transduction, SRC affects various cellular processes, including proliferation, differentiation, motility, and adhesion. It is documented that TGF-β1-induced SRC activation contributes to collagen accumulation and fibrosis through an ERK-dependent pathway[33].

F-actin polymerization is a fundamental mechanism for activating MRTF/SRF and YAP/TAZ signaling. F-actin polymerization leads to the separation of G-actin from MRTF-A, allowing isolated MRTF-A to enter the nucleus and induce fibrotic gene expression in tandem with SRF[34]. Typically, YAP/TAZ is phosphorylated by LATS kinases. However, RhoA-mediated F-actin polymerization can inhibit Lats 1/2 kinase activity and prevent YAP/TAZ phosphorylation. This leads to the translocation of unphosphorylated YAP/TAZ into the nucleus, which promotes fibrosis[35]. Our observations indicated that UC-MSC-CM not only downregulated the expression of MRTF-A and SRF, but also suppressed the expression of RhoA, ROCK1 (albeit not significantly), ROCK2, and SRC. It has been established that SRC activation by TGF-β1 plays a pivotal role in mediating F-actin polymerization, primarily through the stimulation of mDia[32,33,36]. These observations imply that UC-MSC-CM exerts anti-fibrogenic effects by attenuating the Rho/ROCK and TGF-β/SRC signaling pathways. Furthermore, our data revealed that UC-MSC-CM impeded F-actin polymerization in HEFs. The inhibition of F-actin polymerization was intrinsically linked to the suppression of YAP/TAZ activity, which is typically facilitated by the inhibition of LATS 1/2 kinases[37]. In summary, these findings indicate that UC-MSC-CM manifests anti-fibrogenic properties by modulating the TGF-β1 pathway at an upstream level. This modulation results in a comprehensive effect that extends beyond the selective inhibition of MRTF/SRF and YAP/TAZ signaling. Additionally, UC-MSC-CM interferes with the Rho/ROCK pathway, consequently inhibiting F-actin polymerization.

Our findings showed that UC-MSC-CM culture inhibits TGF-β1-mediated fibrogenesis in HEFs, as evidenced by reduced Smad2 phosphorylation. This suggested that the anti-fibrogenic action of UC-MSC-CM may involve Smad-dependent pathways. These results align with our previous observations that UC-MSCs diminish the TGF-β1-induced phosphorylation of both Smad2 and Smad3[18]. Previous research has established that the TGF-β1/Smad2 signaling pathway plays a role in the anti-fibrotic action of UC-MSCs across different organs[20,38,39]. In addition, UC-MSC exosomes, which are enriched in specific microRNAs, show anti-scarring effects by suppressing the TGF-β2/SMAD2 pathway, suggesting their potential to prevent scar formation during wound healing[40]. In the Smad-dependent pathway, TGF-β1 induces the formation of a phosphorylated Smad2/3-Smad4 complex. This complex then translocates to the nucleus, where it activates fibrogenic genes. We found that reduced Smad2 phosphorylation was linked to the UC-MSC-CM-mediated inhibition of YAP/TAZ expression in HEFs. YAP/TAZ is known to interact with the Smads complex, influencing TGF-β1/Smads signaling[11]. Earlier studies have shown that YAP/TAZ knockdown modifies TGF-β receptor activity, leading to a marked decrease in both phosphorylated Smad2/3 and their nuclear localization[41]. The results of this study corroborated our hypothesis that UC-MSC-CM reduces YAP/TAZ expression, subsequently leading to diminished Smad2 phosphorylation. Our study chose the selected time points (24/48 h) to investigate signaling responses to TGF-β1. Koo et al.[6] reported that when fibrosis induced by TGF-β1 is observed, the highest expression of the final fibrosis marker occurs at 48 h. The RNA level (from the Q-PCR experiment) likely reaches its peak before this time. However, TGF-β1 induced fibrogenic activation is regulated by Smad-dependent and Smad-independent TGF-β1 signaling. Since changes often occur during the Smad-dependent in early phase, we examined the Smad2 phosphorylation in the presence of 500 μg/mL UC-MSC-CM at 30 min, 1 h, and 3 h following TGF-β1 treatment. As shown in Fig. S6, Smad2 phosphorylation was observed starting at 30 min after TGF-β1 stimulation and significantly reduced in 1 h after TGF-β1 stimulation.

The limitation of our research was the inability to demonstrate through pathway-specific agonists that the effects of TGF- β1 were restored via the pathways by UC-MSC CM. However, in this study, we initially focused on confirming the anti-fibrotic effect of UC-MSC CM in human embryonic fibroblasts (HEF). In future research, we aim to demonstrate the association of these pathways using pathway-specific agonists. Further, in this study, we did not conduct experiments at earlier time points to capture the optimal responses. In other similar studies[18,42–44], no significant changes in MRTF-A ICC were observed in response to TGF-β1 (colonic/lung fibroblast; 24–48 h). While the exact reason for this remains unclear, considering MRTF-A as a type of signaling molecule, it is possible that changes might occur more prominently in the early phase. However, Sisson et al.[42] also did not show differences even at 24 h, which is earlier than our experimental conditions. Therefore, rather than re-experimenting with MRTF-A at early times, our research team opted to conduct additional experiments using cytosolic/nuclear extract in western blot, a more accurate method for quantifying changes, to clearly demonstrate the quantitative changes in MRTF-A induced by TGF-β1.

In conclusion, our study indicates that human UC-MSC-CM may suppress the TGF-β1-induced fibrogenic activation process in HEFs by targeting both Smad2-dependent and Rho-mediated MRTF/SRF and YAP/TAZ pathways (Fig. 8). This insight opens up new possibilities for the clinical use of UC-MSC-CM in the targeted and effective treatment of esophageal fibrosis, which currently lacks effective therapies. Nonetheless, additional research including studies in vivo, to identify the anti-fibrogenic components of UC-MSC-CM, is essential to confirm these findings and optimize the use of UC-MSC-CM for therapeutic purposes.

Methods

Ethical approval and consent to participate

This study adheres to the Declaration of Helsinki and was approved by Institutional Review Board of the CHA Bundang Medical Center, Korea (Approval number: CHAMC2017-07-021-007). The present IRB number has been approved for the provision of donor tissues for the manufacturing of the investigational material (UC-MSC Cell bank, product name: CordSTEM, manufacturing number: C-M07). Informed consent was obtained from

all participants at the CHA Bundang Medical Center (Seongnam, Korea) prior to the collection of umbilical cords.

Cell culture

HEFs, obtained from ScienCell (HEFs; #2730; Carlsbad, CA, USA) were cultured in poly-L-lysine-coated culture vessels (2μg/cm^2) with Fibroblast Medium (FM; #2301; ScienCell). To induce TGF-β1 stimulation, HEFs were grown until reaching 70–80% confluence, starved for 24 h in serum-free culture medium, followed by treatment with 5 ng/mL of TGF-β1 (R&D System, Minneapolis, MN) for the specified durations.

Preparation of human UC-MSCs

Human UC-MSCs were generously provided by CHA Biotech Co. Ltd. (Seongnam, Korea). The isolation and expansion of these cells followed the protocols in accordance with the Good Clinical Practice guidelines of the Master Cell Bank. Human UC-MSCs underwent preparation at the Good Manufacturing Practices Facility. The process of cell preparation and characterization followed previously established protocols[18,45–47]. After the umbilical vessels were severed, segments of Wharton's jelly were cut into explants measuring 1–5 mm in length to extract UC-MSCs. These isolated slices were affixed to culture plates and then cultured in α-modified minimal essential medium (Hyclone) supplemented with 10% fetal bovine serum (Gibco), 25 ng/mL fibroblast growth factor-4 (Peprotech, London, England), 1 μg/mL heparin (Sigma, St. Louis, MO), and 0.5% gentamycin (Gibco) at 37 °C in a humidified atmosphere containing 5% CO2. The medium was changed every 3 days, and by day 6, UC-MSC populations began to emerge from the explanted UC fragments. After 15 days, the UC fragments were discarded, and the cells were cultured to sub-confluence (80–90%) using TrypLE (Invitrogen, Carlsbad, CA). UC-MSCs at passage six were utilized, following the methodology outlined in our prior publication[18], and their phenotypic characteristics were assessed via fluorescence-activated cell sorting analysis.

Preparation of human UC-MSC-CM

UC-MSCs (1.0×10^6 cells) were plated in a 100 mm dish containing 10 mL of UC-MSC culture medium to produce the conditioned medium (CM). After 24 h, the serum-free HEF culture medium was substituted. Following 72 h of incubation, the CM was collected. To eliminate cellular debris, the CM was centrifuged at 3800×g for 10 min. The resulting supernatant was filtered through a 0.2-μm filter and concentrated 15-fold using a 3-kDa cut-off centrifugal filter (Amicon Ultra, Merck Millipore, Burlington, MA, USA) at 4000×g for 40 min at 4 °C. After that, the protein concentration was measured using the Pierce bicinchoninic acid protein assay kit (Thermo Scientific, #23227).

Culture of HEFs with UC-MSC-CM

To investigate the effects of UC-MSC-CM on TGF-β1-induced fibrosis in HEFs, HEFs, originally cultured in medium supplemented with serum, underwent serum deprivation for 24 h in HEF-specific serum-free medium. Following this, HEFs were exposed to 5 ng/mL of TGF-β1, either independently or in conjunction with UC-MSC-conditioned medium (CM) at concentrations of 100, 250, or 500 μg/mL. This research aimed to explore the influence of UC-MSC-CM on TGF-β1-induced fibrosis in HEFs.

Real-time quantitative polymerase chain reaction (RT-qPCR)

HEFs were seeded at a density of 4×10^4 cells/well on a 6-well culture plate. After serum starvation for 24 h, the cells were treated with 5 ng/ml TGF-β1 and UC-MSC-CM for 24 h. Total RNA was extracted from the HEFs using the TRIzol reagent (Ambion, Carlsbad, CA). Then, an equal amount of RNA (1 μg) was reverse-transcribed into cDNA utilizing the ReverTra Ace qPCR RT Master Mix Kit (TOYOBO, Osaka, Japan), in accordance with the manufacturer's protocol. All RT-qPCR reactions were performed using a Roche Light Cycler 96 instrument (Roche) with Faster-Start Essential DNA Probes Master Mix (Roche). The mRNA levels of all genes were normalized to those of GAPDH. The specific primers for the collagen1A1 (Hs00164004_m1), fibronectin (Hs01549976_m1), α-smooth muscle actin (α-SMA) (ACTA2, Hs00426835_g1), *MKL1* (MRTF-A, Hs01090249_g1), *SRF* (Hs01065256_m1), *RHOA* (Hs00357608_m1), *ROCK1* (Hs01127701_m1), *ROCK2* (Hs00178154_m1), *SRC* (Hs01082246_m1), *YAP1* (Hs00902712_g1), *WWTR1* (Hs00210007_m1), and *GAPDH* (Hs03929097_g1) genes were purchased from Applied Biosystems (Foster City, CA).

Western blotting

HEFs were seeded at a density of 3×10^5 cells on a 100 mm^2 culture dish. After serum starvation for 24 h, the cells were treated with TGF-β1 (5 ng/mL) and UC-MSC-CM for 48 h. Total protein extraction was carried out using RIPA buffer (Cell Signaling Technology, Beverly, MA, USA) supplemented with proteinase and phosphatase inhibitor cocktails. Subsequently, protein concentration was determined using a Pierce bicinchoninic acid protein assay kit (Thermo Scientific, #23227), followed by western blot analysis conducted according to established protocols[24]. Primary antibodies against procollagen1A1 (Procol1A1) (SP1D8, Developmental Studies Hybridoma Bank, Iowa City, IA), fibronectin (FN) (ab2413, Abcam, Cambridge, MA), α-SMA (A2547, Sigma), phospho-Smad2 (Ser465/467) (#3108, Cell Signaling), total-Smad2 (#3102, Cell Signaling), RhoA (#sc-418, Santa Cruz Biotechnology, Dallas, TX), GAPDH (#2118, Cell Signaling), Mkl1(MRTF-A) (21166-1-AP, ProteinTech), SRF (#5147, Cell Signaling), HDAC1 (#5356, Cell Signaling), phospho-YAP (Ser127) (#13008, Cell Signaling), YAP (#sc-101199, Santa Cruz Biotechnology, Dallas, TX), and TAZ (#8418, Cell Signaling) were used.

Extraction of nuclear and cytoplasmic proteins

The separation of nuclear and cytoplasmic fractions from HEFs was achieved utilizing a Nuclear Extraction kit (Millipore), following the manufacturer's instructions. Subsequently, protein concentration was determined employing the bicinchoninic acid protein assay, followed by western blotting.

Immunocytochemistry

Immunofluorescence staining was conducted following established protocols[6,18]. HEFs (1×10^4 cells/well) were seeded onto chamber slides (#30108, SPL Life Sciences, South Korea) and exposed to TGF-β1 (5 ng/mL) and UC-MSC-CM for 48 h. The slides underwent overnight incubation at 4°C with primary antibodies against Procol1A1, FN, α-SMA, MRTF-A, and YAP, followed by a 90 min incubation at room temperature with a fluorescent secondary antibody. LSM880 confocal laser scanning microscope. The nuclear-to-cytoplasmic ratio of MRTF-A and YAP staining was quantified using ImageJ software. Individual cells were outlined using Cell Mask stain, and their optical density was measured and adjusted based on cell area. DAPI staining delineated the nucleus, facilitating the calculation of MRTF-A or YAP staining density within the nucleus. The cytoplasmic fraction was obtained by subtracting the nuclear fraction from the total cell count, and the nuclear-to-cytoplasmic ratio was calculated by dividing the nuclear signal by the cytoplasmic signal. Analysis included an average density measurement from at least 10 cells per image. The fluorescence intensity ratio of F-actin to DAPI was quantitatively analyzed using ImageJ software. Measurements were taken across 21 distinct same sized surface areas (3,900 μm ^{2} for images taken with zoom factor 1) from 3 independent experiments.

Statistical analysis

The data are presented as mean ± standard error of the mean (SEM) from a minimum of three independent experiments. The Mann–Whitney U test was utilized for comparisons between the two groups. For multiple comparisons, analysis of variance (ANOVA) followed by Tukey's post-hoc test was conducted. Statistical significance was set at $P < 0.05$. All statistical analyses were carried out using GraphPad Prism 8.0 software (GraphPad Software, San Diego, CA, USA).

Data availability

All data reported have been obtained from experiments carried out in the author's laboratory. The dataset generated during the present study is available upon reasonable request to the corresponding authors (Prof. In Kyung Yoo or Prof. Jun Hwan Yoo).

Received: 18 March 2024; Accepted: 13 September 2024
Published online: 27 September 2024

References

1. Zhang, Y. et al. Mitomycin C inhibits esophageal fibrosis by regulating cell apoptosis and autophagy via lncRNA-ATB and miR-200b. *Front. Mol. Biosci.* **8**, 675757. https://doi.org/10.3389/fmolb.2021.675757 (2021).
2. Mizushima, T. et al. Oral administration of conditioned medium obtained from mesenchymal stem cell culture prevents subsequent stricture formation after esophageal submucosal dissection in pigs. *Gastrointest. Endosc.* **86**, 542–552e1. https://doi.org/10.1016/j.gie.2017.01.024 (2017).
3. Biancheri, P. et al. The role of transforming growth factor (TGF)-beta in modulating the immune response and fibrogenesis in the gut. *Cytokin Growth Factor Rev.***25**, 45–55. https://doi.org/10.1016/j.cytogfr.2013.11.001 (2014).
4. Derynck, R. & Zhang, Y. E. Smad-dependent and smad-independent pathways in TGF-beta family signalling. *Nature* **425**, 577–584. https://doi.org/10.1038/nature02006 (2003).
5. Mu, Y., Gudey, S. K. & Landström, M. Non-smad signaling pathways. *Cell. Tissue Res.* **347**, 11–20. https://doi.org/10.1007/s00441-011-1201-y (2012).
6. Koo, J. B. et al. Anti-fibrogenic effect of PPAR-γ agonists in human intestinal myofibroblasts. *BMC Gastroenterol.* **17**, 73. https://doi.org/10.1186/s12876-017-0627-4 (2017).
7. Liu, F. et al. Mechanosignaling through YAP and TAZ drives fibroblast activation and fibrosis. *Am. J. Physiol. Lung Cell. Mol. Physiol.* **308**, L344–L357. https://doi.org/10.1152/ajplung.00300.2014 (2015).
8. Mannaerts, I. et al. The Hippo pathway effector YAP controls mouse hepatic stellate cell activation. *J. Hepatol.* **63**, 679–688. https://doi.org/10.1016/j.jhep.2015.04.011 (2015).
9. Martin, K. et al. PAK proteins and YAP-1 signalling downstream of integrin beta-1 in myofibroblasts promote liver fibrosis. *Nat. Commun.* **7**, 12502. https://doi.org/10.1038/ncomms12502 (2016).
10. Seo, E. et al. The Hippo-Salvador signaling pathway regulates renal tubulointerstitial fibrosis. *Sci. Rep.* **6**, 31931. https://doi.org/10.1038/srep31931 (2016).
11. Szeto, S. G. et al. YAP/TAZ are mechanoregulators of TGF-β-Smad signaling and renal fibrogenesis. *J. Am. Soc. Nephrol.* **27**, 3117–3128. https://doi.org/10.1681/ASN.2015050499 (2016).
12. Piccolo, S., Dupont, S. & Cordenonsi, M. The biology of YAP/TAZ: hippo signaling and beyond. *Physiol. Rev.* **94**, 1287–1312. https://doi.org/10.1152/physrev.00005.2014 (2014).
13. Samadi, P., Saki, S., Manoochehri, H. & Sheykhhasan, M. Therapeutic applications of mesenchymal stem cells: a comprehensive review. *Curr. Stem Cell. Res. Ther.* **16**, 323–353. https://doi.org/10.2174/1574888X15666200914142709 (2021).
14. Yin, F., Wang, W. Y. & Jiang, W. H. Human umbilical cord mesenchymal stem cells ameliorate liver fibrosis in vitro and in vivo: from biological characteristics to therapeutic mechanisms. *World J. Stem Cells* **11**, 548–564. https://doi.org/10.4252/wjsc.v11.i8.548 (2019).
15. Musiał-Wysocka, A., Kot, M. & Majka, M. The pros and cons of mesenchymal stem cell-based therapies. *Cell Transpl.***28**, 801–812. https://doi.org/10.1177/0963689719837897 (2019).
16. Røsland, G. V. et al. Long-term cultures of bone marrow–derived human mesenchymal stem cells frequently undergo spontaneous malignant transformation. *Cancer Res.* **69**, 5331–5339. https://doi.org/10.1158/0008-5472.CAN-08-4630 (2009).
17. Walczak, P. et al. Dual-modality monitoring of targeted intraarterial delivery of mesenchymal stem cells after transient ischemia. *Stroke* **39**, 1569–1574. https://doi.org/10.1161/STROKEAHA.107.502047 (2008).

18. Choi, Y. J. et al. Umbilical cord/placenta-derived mesenchymal stem cells inhibit fibrogenic activation in human intestinal myofibroblasts via inhibition of myocardin-related transcription factor A. *Stem Cell. Res. Ther.* **10**, 291. https://doi.org/10.1186/s13287-019-1385-8 (2019).
19. Hou, L. et al. Human umbilical cord mesenchymal stem cell-derived extracellular vesicles alleviated silica induced lung inflammation and fibrosis in mice via circPWWP2A/miR-223–3p/NLRP3 axis. *Ecotoxicol. Environ. Saf.* **251**, 114537. https://doi.org/10.1016/j.ecoenv.2023.114537 (2023).
20. Moodley, Y. et al. Human umbilical cord mesenchymal stem cells reduce fibrosis of bleomycin-induced lung injury. *Am. J. Pathol.* **175**, 303–313. https://doi.org/10.2353/ajpath.2009.080629 (2009).
21. Hinz, B., Celetta, G., Tomasek, J. J., Gabbiani, G. & Chaponnier, C. Alpha-smooth muscle actin expression upregulates fibroblast contractile activity. *Mol. Biol. Cell* **12**, 2730–2741. https://doi.org/10.1091/mbc.12.9.2730 (2001).
22. An, S. Y. et al. Milk fat globule-EGF factor 8, secreted by mesenchymal stem cells, protects against liver fibrosis in mice. *Gastroenterology* **152**, 1174–1186. https://doi.org/10.1053/j.gastro.2016.12.003 (2017).
23. Knipe, R. S., Tager, A. M. & Liao, J. K. The rho kinases: critical mediators of multiple profibrotic processes and rational targets for new therapies for pulmonary fibrosis. *Pharmacol. Rev.* **67**, 103–117. https://doi.org/10.1124/pr.114.009381 (2015).
24. Small, E. M. et al. Myocardin-related transcription factor-a controls myofibroblast activation and fibrosis in response to myocardial infarction. *Circ. Res.* **107**, 294–304. https://doi.org/10.1161/CIRCRESAHA.110.223172 (2010).
25. Makita, R. et al. Multiple renal cysts, urinary concentration defects, and pulmonary emphysematous changes in mice lacking TAZ. *Am. J. Physiol. Ren. Physiol.* **294**, F542–F553. https://doi.org/10.1152/ajprenal.00201.2007 (2008).
26. Mitani, A. et al. Transcriptional coactivator with PDZ-binding motif is essential for normal alveolarization in mice. *Am. J. Respir. Crit. Care Med.* **180**, 326–338. https://doi.org/10.1164/rccm.200812-1827OC (2009).
27. Attisano, L. & Wrana, J. L. Signal integration in TGF-β, WNT, and Hippo pathways. *F1000Prime Rep.* 5, 17 (2013).
28. Nakamura, R., Hiwatashi, N., Bing, R., Doyle, C. P. & Branski, R. C. Concurrent YAP/TAZ and SMAD signaling mediate vocal Fold fibrosis. *Sci. Rep.* **11**, 13484. https://doi.org/10.1038/s41598-021-92871-z (2021).
29. Varelas, X. et al. TAZ controls smad nucleocytoplasmic shuttling and regulates human embryonic stem-cell self-renewal. *Nat. Cell Biol.* **10**, 837–848. https://doi.org/10.1038/ncb1748 (2008).
30. Huh, H. D., Kim, D. H., Jeong, H. S. & Park, H. W. Regulation of TEAD transcription factors in cancer biology. *Cells* **8**, 600. https://doi.org/10.3390/cells8060600 (2019).
31. Zhu, T. et al. YAP/TAZ affects the development of pulmonary fibrosis by regulating multiple signaling pathways. *Mol. Cell. Biochem.* **475**, 137–149. https://doi.org/10.1007/s11010-020-03866-9 (2020).
32. Small, E. M. The actin–MRTF–SRF gene regulatory axis and myofibroblast differentiation. *J. Cardiovasc. Transl. Res.* **5**, 794–804. https://doi.org/10.1007/s12265-012-9397-0 (2012).
33. Mishra, R., Zhu, L., Eckert, R. L. & Simonson, M. S. TGF-β-regulated collagen type I accumulation: role of src-based signals. *Am. J. Physiol. Cell. Physiol.* **292**, C1361–C1369. https://doi.org/10.1152/ajpcell.00370.2006 (2007).
34. Kurose, H. Cardiac fibrosis and fibroblasts. *Cells* **10**, 1716. https://doi.org/10.3390/cells10071716
35. Mosaddad, S. A. et al. Response to mechanical cues by interplay of YAP/TAZ transcription factors and key mechanical checkpoints of the cell: a comprehensive review. *Cell. Physiol. Biochem.* **55**, 33–60. https://doi.org/10.33594/000000325 (2021).
36. Quack, T. et al. The formin-homology protein SmDia interacts with the src kinase SmTK and the GTPase SmRho1 in the gonads of Schistosoma mansoni. *PLoS One* **4**, e6998. https://doi.org/10.1371/journal.pone.0006998 (2009).
37. Wada, K. I., Itoga, K., Okano, T., Yonemura, S. & Sasaki, H. Hippo pathway regulation by cell morphology and stress fibers. *Development* **138**, 3907–3914. https://doi.org/10.1242/dev.070987 (2011).
38. Fang, S. et al. Umbilical cord-derived mesenchymal stem cell-derived exosomal microRNAs suppress myofibroblast differentiation by inhibiting the transforming growth factor-β/SMAD2 pathway during wound healing. *Stem Cells Transl. Med.* **5**, 1425–1439. https://doi.org/10.5966/sctm.2015-0367 (2016).
39. Li, T. et al. Exosomes derived from human umbilical cord mesenchymal stem cells alleviate liver fibrosis. *Stem Cells Dev.* **22**, 845–854. https://doi.org/10.1089/scd.2012.0395 (2013).
40. Bian, D., Wu, Y., Song, G., Azizi, R. & Zamani, A. The application of mesenchymal stromal cells (MSCs) and their derivative exosome in skin wound healing: a comprehensive review. *Stem Cell. Res. Ther.* **13**, 24. https://doi.org/10.1186/s13287-021-02697-9 (2022).
41. Labibi, B., Bashkurov, M., Wrana, J. L. & Attisano, L. Modeling the control of TGF-β/smad nuclear accumulation by the hippo pathway effectors, taz/yap. *iScience* 23, 101416 (2020). https://doi.org/10.1016/j.isci.2020.101416
42. Sisson, T. H. et al. Inhibition of myocardin-related transcription factor/serum response factor signaling decreases lung fibrosis and promotes mesenchymal cell apoptosis. *Am. J. Pathol.* **185**, 969–986. https://doi.org/10.1016/j.ajpath.2014.12.005 (2015).
43. Johnson, L. A. et al. Novel Rho/MRTF/SRF inhibitors block matrix-stiffness and TGF-β–induced fibrogenesis in human colonic myofibroblasts. *Inflamm. Bowel Dis.* **20**, 154–165 (2014).
44. Choi, Y. J., Kim, W. R., Kim, D. H., Kim, J. H. & Yoo, J. H. Human umbilical cord/placenta mesenchymal stem cell conditioned medium attenuates intestinal fibrosis in vivo and in vitro. *Stem Cell Res. Ther.* **15**, 69 (2024).
45. Kho, A. R. et al. Administration of placenta-derived mesenchymal stem cells counteracts a delayed anergic state following a transient induction of endogenous neurogenesis activity after global cerebral ischemia. *Brain Res.* **1689**, 63–74. https://doi.org/10.1016/j.brainres.2018.03.033 (2018).
46. Kim, M. J. et al. Human chorionic-plate-derived mesenchymal stem cells and Wharton's jelly-derived mesenchymal stem cells: a comparative analysis of their potential as placenta-derived stem cells. *Cell. Tissue Res.* **346**, 53–64. https://doi.org/10.1007/s00441-011-1249-8 (2011).
47. Oh, S. H. et al. Interleukin-1 receptor antagonist-mediated neuroprotection by umbilical cord-derived mesenchymal stromal cells following transplantation into a rodent stroke model. *Exp. Mol. Med.* **50**, 1–12. https://doi.org/10.1038/s12276-018-0041-1 (2018).

Acknowledgements

This work was supported by the National Research Foundation of Korea (NRF) grant funded by The Ministry of Science and ICT (NRF-2021R1F1A1061550, NRF-2020R1F1A1066323) and Korea government (MSIT; No. RS-2022-00165708). The funding body played no role in the design of the study and collection, analysis, and interpretation of data and in writing the manuscript.

Author contributions

YJC, JHK, YL, HJP, IKY, and JHY performed the experiments. YJC, YL, and JHK analyzed the data. IKY and JHY designed the research. YJC and IKY drafted the manuscripts. JHK and JHY edited and revised the manuscript. IKY and JHY did a critical revision of the manuscript and supervised the study. All authors read and approved the final manuscript.

Declarations

Competing interests
The authors declare no competing interests.

Additional information
Supplementary Information The online version contains supplementary material available at https://doi.org/10.1038/s41598-024-73091-7.

Correspondence and requests for materials should be addressed to I.K.Y. or J.H.Y.

Reprints and permissions information is available at www.nature.com/reprints.

Publisher's note Springer Nature remains neutral with regard to jurisdictional claims in published maps and institutional affiliations.